Check for updates

ADVANCED THERAPEUTICS
www.advtherap.com

Survivin-Based Recombinant Overlapping Peptides Induce T Lymphocyte Cytotoxicity and Prolong the Survival in In Vivo Melanoma Model

Yuanting Zhang, Yihan Zhou, Min Gong, Qing Zhang, Qiujie Zheng, Yuanying Shen, Wenshu Lu,* and Shisong Jiang**

Anti-cancer vaccination emerged as a promising and cost-effective immunotherapy, but the lack of immunogenicity has hindered the success of therapeutic vaccine development. To address this issue and improve therapeutic efficacy, this study presents the examination of recombinant overlapping peptides (ROP) based on the tumor-associated antigen, survivin, on in vivo immunogenicity and anti-tumor efficacy using a melanoma C57/BL mouse model. Results show that ROPs induce a remarkable 46.5% cytotoxic activity mediated by activated cytotoxic T lymphocytes, compared to only 3% in wild-type (WT) survivin protein. Additionally, ROPs significantly reduce tumor size by over 500 mm^3 and prolong survival rates in mice with zero deaths in the first 17 days and 30% survival at the end of day 23, while no mice immunized with WT survivin protein survive beyond day 20. ROPs combined with anti-4-1BB agonists lead to additional tumor size reduction by 500 mm^3 and 70% survival on day 23. These findings underscore the importance of survivin as a trigger for tumor-restricting immunity and provide therapeutic evidence of ROPs' anti-tumor potential, especially when combined with other immunostimulants, such as anti-4-1BB agonists. ROPs and adjuvant immunostimulants represent a potent vaccine strategy for therapeutic purposes, increasing vaccine immunogenicity and improving survival against cancer.

1. Introduction

Cancer is a leading cause of mortality worldwide, with millions of new cases and deaths each year.[1] While conventional treatments like surgery, radiation, and chemotherapy have been available, immunotherapy has emerged as a potent option for patients with advanced metastasis or resistance to other therapies.[2] Among different immunotherapeutic strategies, cancer vaccines offer a safe, cost-effective, and promising option. Peptide-based cancer vaccines use epitope peptides from tumor-specific (TAA) or associated antigens (TSA) to guide the immune system to target antigen-specific tumor tissues.[3,4] Multiple epitopes derived from TAA have been identified and evaluated as vaccine peptides that are currently under ongoing clinical investigations, especially those for anti-cancer treatments.[5,6]

Although epitope-based vaccines are considered an attractive strategy for cancer vaccines, there are several concerns associated with their implementation. One major challenge is the time-consuming and intricate process of identifying the specific epitope and the corresponding major histocompatibility complex (MHC) molecule that

Y. Zhang, Y. Shen
Department of Medical Microbiology and Immunology
College of Basic Medicine
Dali University
Dali, Yunnan 671003, China
E-mail: yuanyingshen@dali.edu.cn

Y. Zhou, W. Lu, S. Jiang
Department of Oncology
Medical Sciences Division
Old Road Campus Research Building
University of Oxford
Roosevelt Drive, Headington, Oxford OX3 7DQ, UK
E-mail: wenshu.lu@oncology.ox.ac.uk; shisong.jiang@oncology.ox.ac.uk

M. Gong
Department of Pharmacy
Tianjin Medical University
22 Qixiangtai Road, Heping, Tianjin 300070, China

Q. Zhang, Q. Zheng, W. Lu, S. Jiang
Oxford Vacmedix (Changzhou) Co Ltd
7 Hanshan Road, Changzhou, Jiangsu 213125, China

W. Lu, S. Jiang
Shanghai JW Inflinhix Co Ltd
800 Naxian Road, Shanghai 201210, China

The ORCID identification number(s) for the author(s) of this article can be found under https://doi.org/10.1002/adtp.202300253

© 2023 The Authors. Advanced Therapeutics published by Wiley-VCH GmbH. This is an open access article under the terms of the Creative Commons Attribution-NonCommercial-NoDerivs License, which permits use and distribution in any medium, provided the original work is properly cited, the use is non-commercial and no modifications or adaptations are made.

DOI: 10.1002/adtp.202300253

presents it.[7] Furthermore, due to the MHC restriction, single epitope-based vaccines only exhibit efficacy in a limited population with MHC compatibility. To overcome these limitations of epitope-based vaccines, we have been pioneers in the field of utilizing overlapping synthetic peptides (OSP) and recombinant overlapping peptides (ROP) as vaccines.[8,9] Through our extensive research, we have consistently demonstrated that OSP and ROP offer significant advantages over single epitope-based vaccines and wild-type (WT) protein-based vaccines. While single epitopes can only stimulate either CD4+ or CD8+ T cells (but not both), depending on the specific MHC molecule involved,[7] OSP/ROP possess a remarkable ability to be presented by multiple MHC molecules, effectively stimulating both CD4+ and CD8+ T cells.[8–11] This unique characteristic distinguishes OSP and ROP from the single epitope vaccine approach, making them highly promising in the field. Furthermore, our research has consistently indicated that OSP and ROP outperform WT-protein-based vaccines in stimulating both CD4+ and CD8+ T cells[9,10] (Figures S1 and S2, Supporting Information). These findings emphasize the substantial potential of OSP and ROP as highly effective immunization strategies.

Survivin (SVN), a tumor-associated antigen, is overexpressed in 90% of cancers and has been identified as a potential target for anti-cancer vaccination.[12–14] SVN is encoded by the *Baculoviral IAP Repeat Containing 5* (*BIRC5*) gene, which is located on chromosome 17 (17q25.3).[15] SVN belongs to the inhibitor of apoptosis (IAP) family, which is known for protecting cells from death by blocking caspases.[16] Over the past two decades, numerous research studies and clinical trials have demonstrated the effectiveness of SVN-based vaccinations in patients diagnosed with a variety of cancers, including melanoma,[17–19] glioblastoma,[20,21] head and neck squamous cell carcinoma,[22–24] mesothelioma,[25,26] ovarian carcinoma,[27,28] and liver hepatocellular carcinoma.[27,28]

Despite the effectiveness of SVN-based vaccinations in several cancer types, the lack of immunogenicity has hindered the development of successful therapeutic vaccines.[29] To address this issue and improve therapeutic efficacy, we designed a ROP vaccine based on SVN. ROP-SVN vaccines can stimulate both CD4+ and CD8+ T cell immunity,[10] and these findings were consistent with other studies.[8,30] In our previous research, however, we employed a prophylactic immunity model in which immunization of the vaccine was before tumor inoculation.

As part of a comprehensive series of preclinical studies, our objective is to compare the capacity of WT-SVN and ROP-SVN to stimulate T cells. Initially, we will utilize an online database to predict MHC class I and MHC class II binding epitopes from the two vaccine candidates, WT-SVN and ROP-SVN. Furthermore, our study aims to evaluate the therapeutic potential of the ROP-SVN vaccine in a tumor model where the vaccine will be administered after the tumor has started to grow. In order to enhance the immune response, we will also assess the combination of ROP vaccines with a 4-1BB agonist, another immunostimulant agent. By conducting these investigations, we hope to gain valuable insights into the comparative efficacy and potential synergistic effects of ROP-SVN and the 4-1BB agonist in stimulating an immune response.

2. Results

2.1. Pan-Cancer Expression Landscape of *BIRC5* Gene via Bioinformatics

We conducted a bioinformatics analysis using the UCSC Xena tool to compare data from The Cancer Genome Atlas (TCGA) and the Genotype-Tissue Expression (GTEx) databases,[31,32] and investigated the expression of the *BIRC5* gene in cancer tissues. Our analysis showed that *BIRC5* expression varied across 33 types of common human cancers. We found that *BIRC5* expression was significantly higher ($P < 0.001$) than in adjacent normal tissues in all cancer types examined, except for mesothelioma, sarcoma, and uveal melanoma where data was unavailable for comparison (**Figure 1**). These findings indicated that *BIRC5* was expressed in most cancer tissues and could be a potential therapeutic target, based on which an SVN-based cancer therapeutic vaccine was further explored.

2.2. Immune Epitope Prediction for WT-SVN and ROP-SVN

ROP-SVN, which is derived from WT-SVN, exhibits a low level of homology with its parent sequence. This suggests that the T cell epitope profiles of these two vaccine candidates are likely to differ significantly. Therefore, it becomes crucial to analyze their MHC binding epitopes to gain a preliminary understanding of their respective capacities to stimulate T cells.

By analyzing the MHC binding epitopes, we can gain valuable insights into the potential variations in T cell activation and the subsequent immune response induced by ROP-SVN compared to WT-SVN. This analysis will play a critical role in providing essential information for the evaluation and comparison of the immunogenicity of these two vaccine candidates.

To predict the binding potential of WT-SVN and ROP-SVN sequences to MHC class I and II, we employed the Immune Epitope Database (IEDB, https://www.iedb.org/). We considered all sequences with prediction scores greater than 0.2 for MHC class I epitope prediction and 0.1 for MHC class II epitope prediction.

Figure 2a illustrates the results, showing 9 MHC class I epitopes (3 H-2-Db and 6 H-2-Kb) identified for WT-SVN. In contrast, ROP-SVN exhibited a significantly higher number of 21 epitopes (5 H-2-Db and 16 H-2-Kb). While 6 epitopes targeted the inserted enzyme substrate sequence in conjunction with the wild-type sequence, 15 epitopes originated solely from the wild-type sequences. This suggests that ROP-SVN has the potential to elicit a stronger response from MHC class I-restricted T cells (Figure 2a).

In the analysis of MHC class II (H-2-IAb) epitopes, WT-SVN generated only two epitopes, while ROP-SVN displayed a more extensive repertoire of eight epitopes. Notably, among these epitopes, six originated from the inserted enzyme substrate sequence combined with the wild-type sequence. The CD4+ T cells stimulated by either the wild-type or the non-wild-type derived epitopes of ROP-SVN, will contribute significantly to the overall immunogenicity against SVN (Figure 2b).

These findings indicate that ROP-SVN possesses a broader range of epitopes, potentially leading to a more robust activation of MHC class II-restricted T cells, compared to WT-SVN. These analyses contribute to our understanding of the immunogenic

© 2023 The Authors. Advanced Therapeutics published by Wiley-VCH GmbH

23663987, 0, Downloaded from https://onlinelibrary.wiley.com/doi/10.1002/adtp.202300253 by Test, Wiley Online Library on [23/08/2023]. See the Terms and Conditions (https://onlinelibrary.wiley.com/terms-and-conditions) on Wiley Online Library for rules of use; OA articles are governed by the applicable Creative Commons License

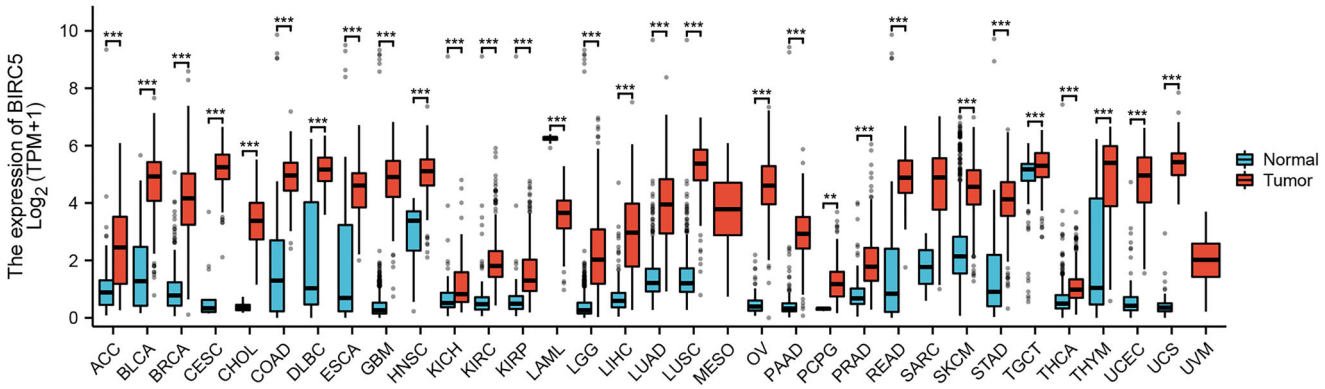

Figure 1. High expression level of *BIRC5* in human tumors. Box plot representation of *BIRC5* expression level in 33 cancer types from TCGA datasets, compared to the corresponding normal tissues from GTEx datasets. $*p < 0.05$; $**p < 0.01$; $***p < 0.001$. ACC: adrenocortical carcinoma ($n = 77$; 122 for normal); BLCA: bladder urothelial carcinoma ($n = 407$; 28 for normal); BRCA: breast invasive carcinoma ($n = 1099$; 292 for normal); CESC: cervical squamous cell carcinoma ($n = 306$; 13 for normal); CHOL: cholangiocarcinoma ($n = 36$; 9 for normal); COAD: colon adenocarcinoma ($n = 290$; 349 for normal); DLBC: lymphoid neoplasm diffuse large B cell lymphoma ($n = 47$; 444 for normal); ESCA: esophageal carcinoma ($n = 182$; 666 for normal); GBM: glioblastoma ($n = 166$; 1157 for normal); HNSC: head and neck squamous cell carcinoma ($n = 520$; 44 for normal); KICH: kidney chromophobe ($n = 66$; 53 for normal); KIRC: kidney renal clear cell carcinoma ($n = 531$; 100 for normal); KIRP: kidney renal papillary cell carcinoma ($n = 289$; 60 for normal); LAML: acute myeloid leukemia ($n = 173$; 70 for normal); LGG: brain lower grade glioma ($n = 523$; 1152 for normal); LIHC: liver hepatocellular carcinoma ($n = 371$; 160 for normal); LUAD: lung adenocarcinoma ($n = 515$; 347 for normal); LUSC: lung squamous cell carcinoma ($n = 498$; 338 for normal); MESO: mesothelioma ($n = 87$); OV: ovarian serous cystadenocarcinoma ($n = 427$; 88 for normal); PAAD: pancreatic adenocarcinoma ($n = 179$; 171 for normal); PCPG: pheochromocytoma and paraganglioma ($n = 182$; 3 for normal); PRAD: prostate adenocarcinoma ($n = 496$; 152 for normal); READ: rectum adenocarcinoma ($n = 93$; 318 for normal); SARC: sarcoma ($n = 262$; 2 for normal); SKCM: skin cutaneous melanoma ($n = 469$; 813 for normal); STAD: stomach adenocarcinoma ($n = 414$; 210 for normal); TGCT: testicular germ cell tumors ($n = 154$; 165 for normal); THCA: thyroid carcinoma ($n = 338$; 512 for normal); THYM: thymoma ($n = 119$; 446 for normal); UCEC: uterine corpus endometrial carcinoma ($n = 181$; 101 for normal); UCS: uterine carcinosarcoma ($n = 57$; 78 for normal); UVM: uveal melanoma ($n = 79$).

differences between WT-SVN and ROP-SVN and highlight the potential of ROP-SVN to stimulate a more diverse and vigorous T cell response.

2.3. Generation of the B16-SVN Cell Line and the Production of ROP-SVN and WT-SVN

To establish a mouse melanoma model, we incorporated the human survivin (hSVN) gene into green fluorescent protein (GFP)-tagged plasmids and transfected them into the murine melanoma B16 cell line. Cells expressing high levels of GFP under an inverted fluorescence microscope were considered transfected cells and were further screened for hSVN overexpression induced by plasmid transfection (**Figure 3**a). Polymerase chain reaction (PCR) (Figure 3b, left) and Western blot (Figure 3b, right) were performed to verify the mRNA and protein expressions of hSVN, respectively. Cells with higher mRNA and protein levels than WT B16-F10 cells were identified as B16-SVN cells that could stably express SVN proteins and could grow melanoma tumors in mice.

The sequence designs for both WT-SVN and ROP-SVN peptides were derived from the hSVN protein sequence. Unlike WT-SVN, which was coded by the recombinant sequence of the hSVN protein, ROP-SVN was designed to include a sequence of 9 LRMK-interspaced peptides, each consisting of 35 amino acids, with 10 amino acids overlapping with its adjacent peptides until the complete sequence of the hSVN protein was included (Figure 3c). The Cathepsin S substrate sequence (LRMK) was interspersed between each peptide. We expressed ROP-SVN and WT-SVN using engineered E. coli BL21 (DE3) cells, purified them by Ni NTA affinity chromatography, and confirmed their expression by SDS-PAGE analysis (Figure 3d). WT-SVN had a single band at 22.0 kDa, which corresponded to its accurate molecular weight, while ROP-SVN had a band at 31–43 kDa, confirming its expression.

2.4. ROP-SVN/Monophosphate Lipid A (MPL) Elicits Stronger SVN-Specific Cytotoxic T Lymphocytes (CTL) Immunity in the Tumor-Free Model

To compare the cellular and humoral immune responses induced by ROP-SVN or WT-SVN proteins emulsified with the adjuvant monophosphate lipid A (MPL), groups of mice were immunized with ROP-SVN/MPL, WT-SVN/MPL, MPL alone, or phosphate-buffered saline (PBS) (**Figure 4**a). The results showed that both ROP-SVN and WT-SVN increased the frequency of antigen-specific interferon(IFN)-γ-secreting T cells. However, in mice immunized with ROP-SVN/MPL, this frequency was ≈0.5 and 10 times higher than that in mice given WT-SVN/MPL and MPL alone ($P < 0.01$), respectively (Figure 4b). All titers for anti-SVN antibodies that reached an optical density (OD) value of 0.2 were detected as 10^5 in response to ROP-SVN/MPL immunization, with no statistical significance compared to WT-SVN/MPL, which led to titers of 8.2×10^4. In the MPL group, there was no detectable antibody (Figure 4c). To further investigate the cellular immunity induced by different immunization approaches, cytotoxic T lymphocytes (CTL)-mediated cytotoxicity was assessed by mixing immunized splenocytes (effector cells) with B16-SVN cells (target cells) and was indicated by lactate dehydrogenase (LDH) release. ROP-SVN/MPL

© 2023 The Authors. Advanced Therapeutics published by Wiley-VCH GmbH

23663987, 0, Downloaded from https://onlinelibrary.wiley.com/doi/10.1002/adtp.202300253 by Test, Wiley Online Library on [23/08/2023]. See the Terms and Conditions (https://onlinelibrary.wiley.com/terms-and-conditions) on Wiley Online Library for rules of use; OA articles are governed by the applicable Creative Commons License

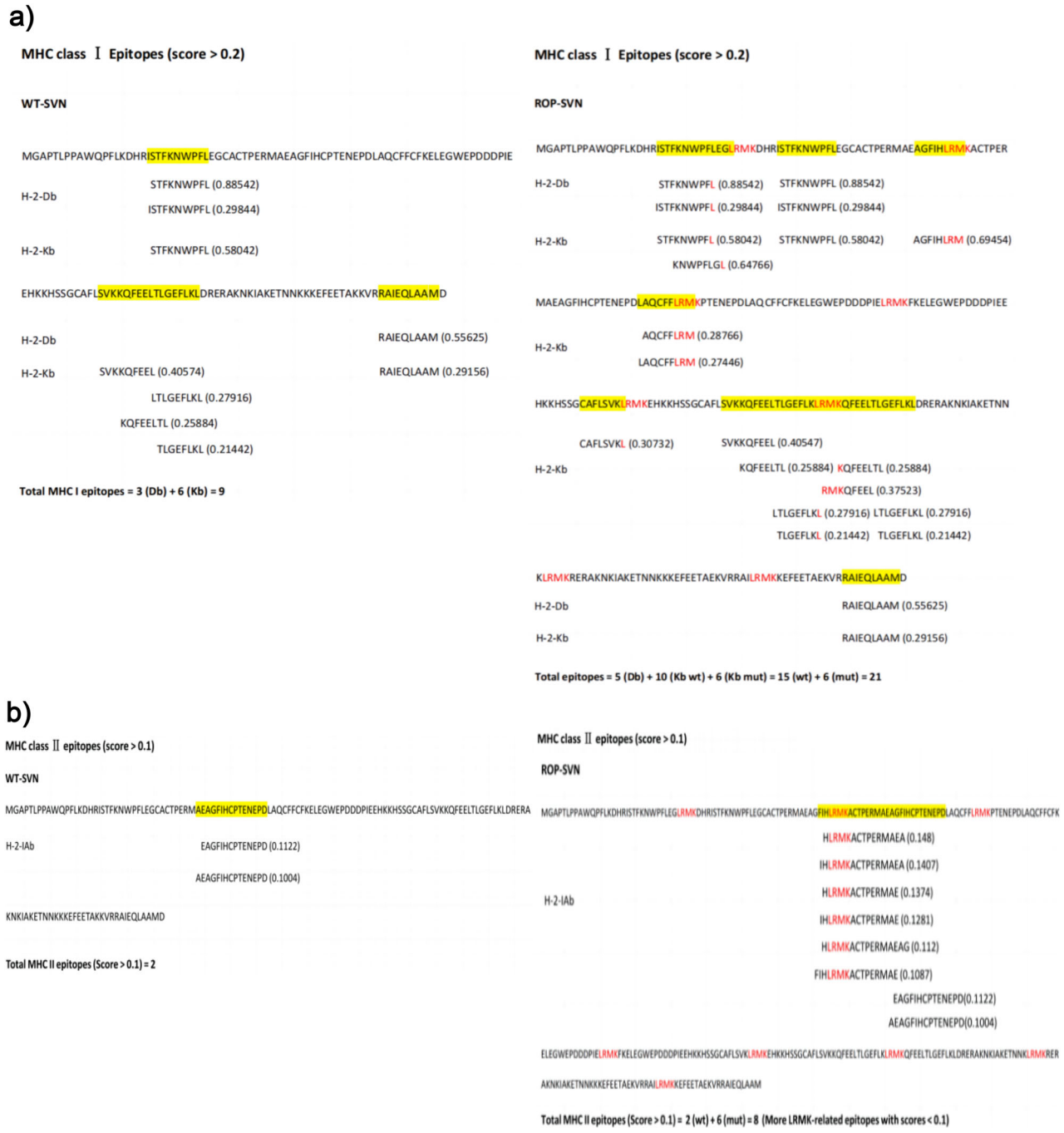

Figure 2. Immune epitope prediction of ROP-SVN and WT-SVN peptides for mouse MHC class I (a) and II (b). a) Epitopes binding to mouse MHC class I (H-2-Db and H-2-Kb) with prediction score > 0.2. b) Epitopes binding to mouse MHC class II (H-2-IAb) with prediction score > 0.1.

immunization resulted in a percentage cytotoxicity of 46.5%, which was significantly higher than that induced by WT-SVN/MPL ($P < 0.0001$) and MPL ($P < 0.001$), which reached 3.1% and 9.5%, respectively, when the effector cell-to-target cell (E:T) ratio was 100:1 (Figure 4d, left). When the E:T ratio was 50:1, the significance remained compared to WT-SVN/MPL ($P < 0.001$) or MPL ($P < 0.01$) (Figure 4d, right). These results suggest that ROP-SVN/MPL can elicit stronger SVN-specific cytotoxic T-cell immunity than WT-SVN/MPL and MPL alone.

2.5. ROP-SVN/MPL has a Significant Anti-Tumor Effect in the B16-SVN Bearing Model

This experiment aimed to assess the ROP-induced immunity in tumor bearing model. After introducing B16-SVN cells to develop melanoma tumors in vivo, C57/BL mice were vaccinated as described in **Figure 5**a. The tumor size was monitored and presented a significantly lower tumor volume of ≈331 mm^3 on day 14 when treated with ROP-SVN/MPL compared to an

© 2023 The Authors. Advanced Therapeutics published by Wiley-VCH GmbH

23663987, 0, Downloaded from https://onlinelibrary.wiley.com/doi/10.1002/adtp.202300253 by Test, Wiley Online Library on [23/08/2023]. See the Terms and Conditions (https://onlinelibrary.wiley.com/terms-and-conditions) on Wiley Online Library for rules of use; OA articles are governed by the applicable Creative Commons License

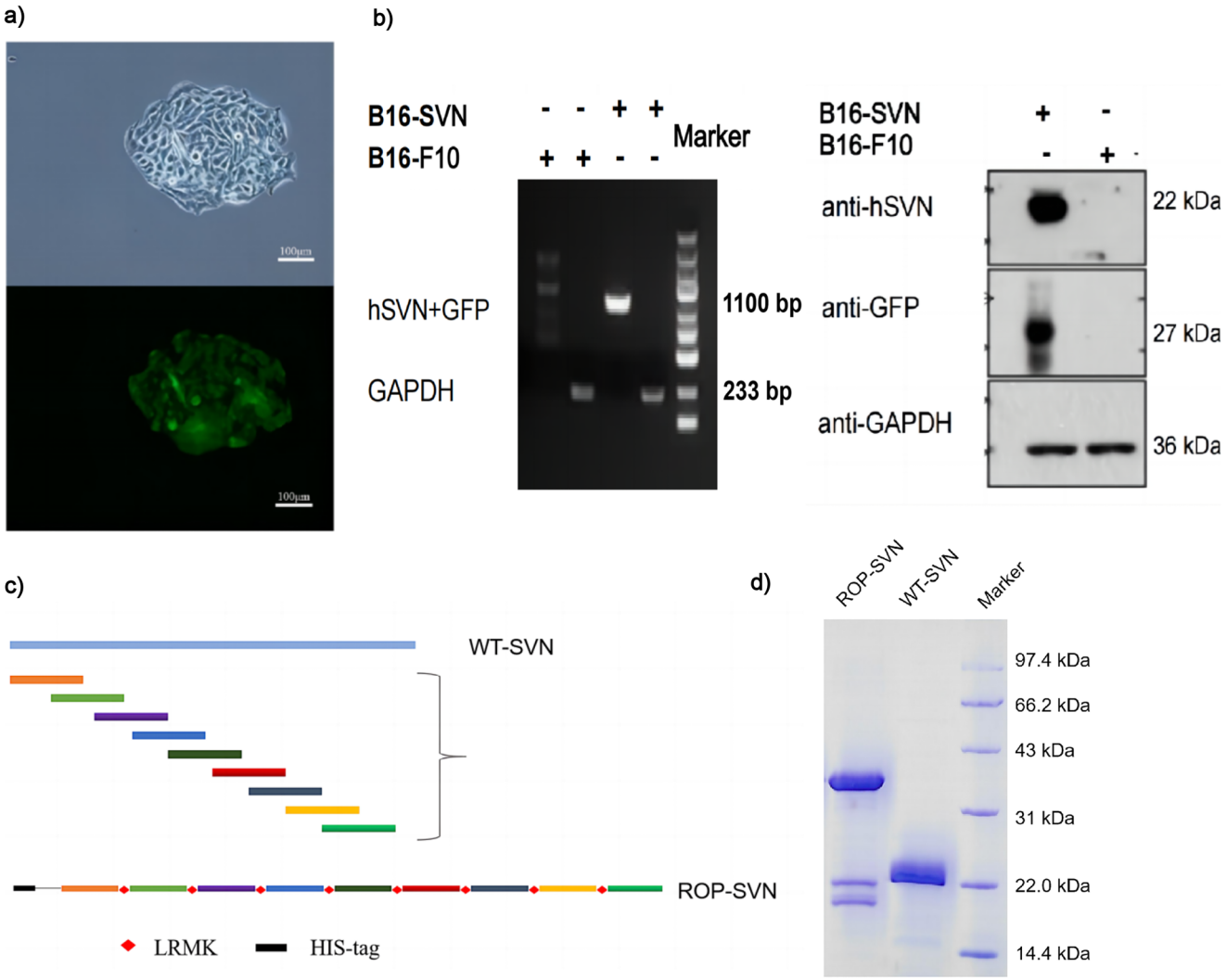

Figure 3. Establishment of B16-SVN melanoma cells a,b) and generation of ROP-SVN and WT-SVN peptides c,d). a) Representative image of GFP-expressing B16-SVN cell colony after transfection seen in cell colony under 200× inverted fluorescence microscope. b) Verification of hSVN expression in B16-SVN cells at genetic levels tested by PCR (left) and protein levels tested by Western blot (right). GAPDH served as a loading control and B16-F10 cells were examined as negative controls. c) Schematic diagram of ROP-SVN design. The WT-SVN sequence is colored in top blue and the shorter colorful sequences below are the 35-amino-acid peptides which overlap each other for 10 amino acids at the ends and cover the full WT-SVN sequence. The bottom long sequence represents the composition of the ROP-SVN sequence where the overlapping peptides are led by a His-tag gene, used for purification, and interspaced by 4 amino acids, LRMK. d) Expression of ROP-SVN and WT-SVN extracted from modified *E. coli* BL-21 (DE3) cells as shown in an SDS-PAGE gel, after purification by a Ni-NTA affinity column.

average tumor volume of ≈990, 930, or 960 mm^3 when treated with WT-SVN/MPL ($P < 0.01$), MPL only ($P < 0.05$), or PBS ($P < 0.01$), respectively (Figure 5b). In addition, mice immunized with ROP-SVN/MPL maintained a tumor volume of up to 722 mm^3 for the next three days (Figure 5b), but the statistical analysis was lacking as more than half of the mice in the three other immunization groups failed to survive (Figure 5c). All mice immunized with WT-SVN/MPL, MPL, or PBS either exceeded or approached the ethical limit of tumor growth on day 20, three days earlier than those immunized with ROP-SVN/MPL (Figure 5b). Correspondingly, a percentage survival of 100% was strikingly maintained if ROP-SVN/MPL was administered before the first 17 days and then dropped to 30% on day 23 for ethical sacrifice (Figure 5c), when no mice were still alive on day 20 after administration of other vaccinations that included WT-SVN/MPL ($P < 0.01$), MPL ($P < 0.001$), and PBS ($P < 0.0001$).

To evaluate whether the improved survival was associated with cellular responses induced by immunization, Figure 5d showed that ROP-SVN evoked a significantly 2-, 4-, and 8-times higher frequency of antigen-specific IFN-γ-secreting T cells in mice than WT-SVN/MPL ($P < 0.01$), MPL ($P < 0.001$), and PBS ($P < 0.0001$), respectively. The average titer that was positive for anti-SVN antibodies (OD value > 0.2) was discovered to be 9.1×10^4 after ROP-SVN/MPL immunization, without significant difference from titers of 6.4×10^4 discovered after WT-SVN/MPL treatment. There were no detectable titers discovered in MPL or PBS control (Figure 5e).

© 2023 The Authors. Advanced Therapeutics published by Wiley-VCH GmbH

23663987, 0, Downloaded from https://onlinelibrary.wiley.com/doi/10.1002/adtp.202300253 by Test, Wiley Online Library on [23/08/2023]. See the Terms and Conditions (https://onlinelibrary.wiley.com/terms-and-conditions) on Wiley Online Library for rules of use; OA articles are governed by the applicable Creative Commons License

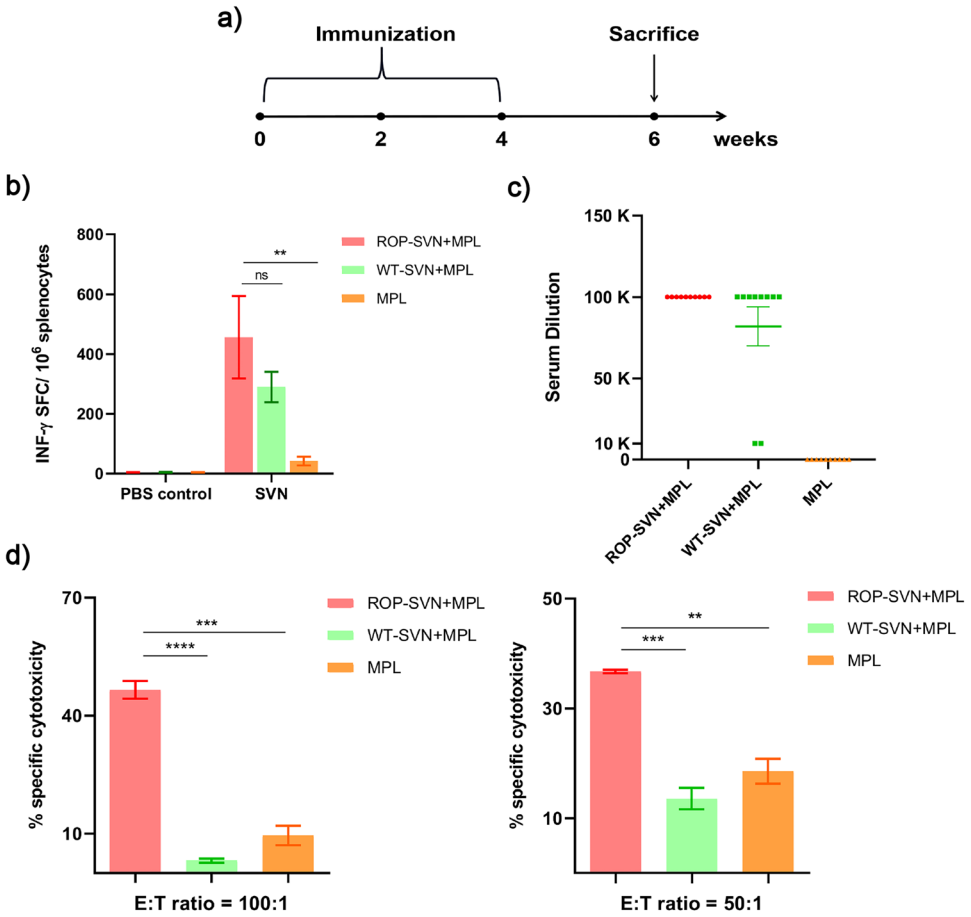

Figure 4. Evaluation of immune responses in mice after immunization. a) Schematic plan for immunization in mice. Ten C57/BL mice were immunized by ROP-SVN/MPL, WT-SVN/MPL, MPL and PBS three times at 2-week intervals and sacrificed for experiments 2 weeks after the last immunization. b) The frequency of IFN-γ-producing T cells was measured by ELISpot after splenocytes of immunized mice (N = 4) were stimulated by SVN or PBS control. c) Titers of anti-SVN antibodies in mice serum (N = 10) as indicated by optical density (OD) values that were greater than 0.2 measured under 450 nm. d) Percentage cytotoxic T lymphocyte activity (N = 6) measured by LDH release at E:T of 100:1 (left) and 50:1 (right). Statistical analysis was performed by comparing ROP-SVN/MPL to WT-SVN/MPL, MPL and PBS. *$p < 0.05$; **$p < 0.01$; ***$p < 0.001$; ****$p < 0.0001$; ns, not significant. All data were presented as mean ± SEM.

Antigen expression in tumor tissue plays a critical role in immune recognition. To investigate whether antigen expression differed across groups, we quantified survivin expression and normalized it to tumor size, comparing tumors smaller and larger than 1000 mm^3. While the average survivin expression in tumors of the ROP-SVN/MPL immunized group (2328 ng per tumor gram) was significantly higher than the PBS control ($p < 0.05$), it was not statistically significantly higher compared to WT-SVN/MPL and MPL (Figure 5f, left). We further investigated whether survivin expression was different in tumors of varying sizes. Strikingly, small tumors (< 1000 mm^3) exhibited 2-to-3-fold higher survivin expression than large tumors (> 1000 mm^3) following ROP-SVN/MPL ($p < 0.01$) and WT-SVN/MPL ($p < 0.01$) immunizations (Figure 5f, right). This result suggested that antigen expression in tumor tissue is negatively correlated with tumor growth in vaccine-immunized mice. The higher the expression of the antigen, the more visible it becomes as a target for the immune system.

2.6. A Combination of ROP-SVN with Anti(α)−4-1BB Agonist Achieves Greater Efficacy

To improve the effectiveness of immunization, we explored a tumor inoculation-immunization model that included an anti(α)−4-1BB agonist monoclonal antibody in the administration plan, as depicted in **Figure 6**a. Combining the α−4-1BB antibody with vaccinations resulted in a significant reduction in tumor volume by more than 500 mm^3 compared to treatment with ROP-SVN/MPL alone ($p < 0.05$) or MPL/α−4-1BB ($p < 0.05$) on day 23, or treatment with MPL alone ($p < 0.05$) on day 20 (see Figure 6b). However, since less than half of the mice in the MPL group survived beyond day 20, or day 23 if treated with ROP-SVN/MPL or α−4-1BB/MPL (as shown in Figure 6c), we were unable to perform a statistical analysis due to the lack of follow-up data (as indicated in Figure 6b).

The pattern of percentage survival observed after α−4-1BB/MPL treatment was identical to that observed after ROP-SVN/MPL treatment before day 23, and all mice groups were

© 2023 The Authors. Advanced Therapeutics published by Wiley-VCH GmbH

23663987, 0, Downloaded from https://onlinelibrary.wiley.com/doi/10.1002/adtp.202300253 by Test, Wiley Online Library on [23/08/2023]. See the Terms and Conditions (https://onlinelibrary.wiley.com/terms-and-conditions) on Wiley Online Library for rules of use; OA articles are governed by the applicable Creative Commons License

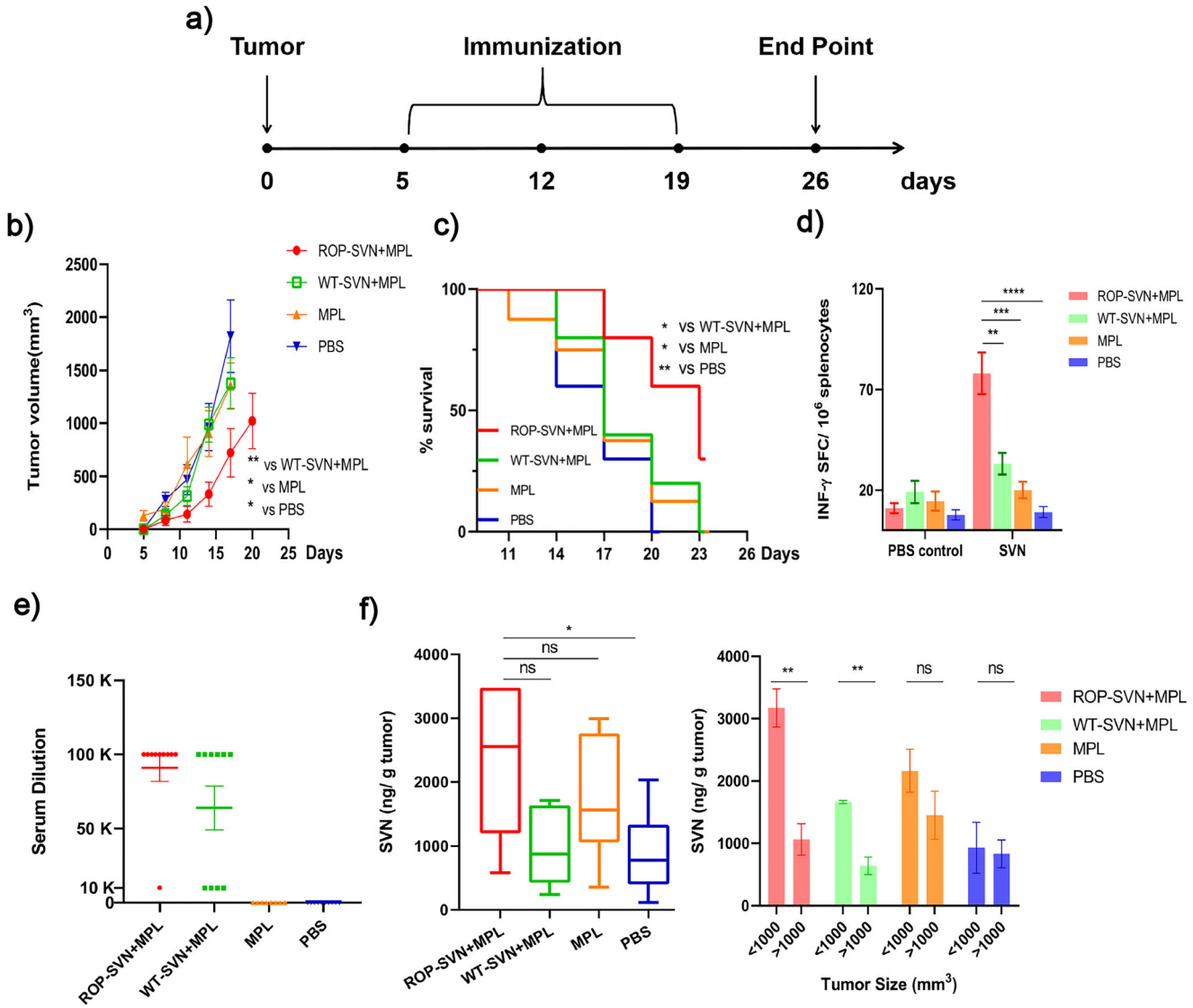

Figure 5. Evaluation of rescue from melanoma tumors in mice after immunization. a) Schematic plan of immunization in melanoma-bearing mice. Ten C57/BL mice were introduced with B16-SVN cells to develop melanoma tumors in vivo and immunized by ROP-SVN/MPL, WT-SVN/MPL, MPL and PBS three times on day 5, 12 and 19 and sacrificed no later than 4 weeks after the induction of tumors by B16-SVN cells. b) Measurement of tumor volumes, in mm^3, every 3 days after immunization until day 20 due to tumor growth exceeding the ethical limit of 1500 mm^3. Mice (N = 10, except for N = 8 in MPL treatment due to failure of tumor modelling) immunized with ROP-SVN/MPL were statistically compared with the other three groups on day 14 before half of any mice group was lethal. c) Monitoring of percentage survival of mice in (b) till day 23 as presented in a Kaplan–Meier plot. d) Measurement of frequency of IFN-γ-producing T cells by ELISpot after splenocytes of melanoma-bearing mice (N = 4) were stimulated by SVN or PBS control. e) Titers of anti-SVN antibodies in the serum of mice in (b), as indicated by optical density (OD) values that were greater than 0.2 measured under 450 nm. f) Quantification of SVN expression in tumors, in ng per tumor gram, of immunized mice in another independent experiment (N = 10), which were classified by tumors > 1000 mm^3 as large tumors and vice versa. Statistical analysis was performed by comparing ROP-SVN/MPL to WT-SVN/MPL, MPL and PBS. *$p < 0.05$; **$p < 0.01$; ***$p < 0.001$; ****$p < 0.0001$; ns, not significant. All data were presented as mean ± SEM.

sacrificed due to ethical limits on day 23 (refer to Figure 6c). Before ethical sacrifice, mice immunized with ROP-SVN/MPL/α−4-1BB maintained over 50% survival and experienced a lower decrease in percentage survival by 30% until day 23, compared to those treated with ROP-SVN/MPL (70%), α−4-1BB/MPL, or MPL (90%) ($p < 0.01$) (see Figure 6c).

In summary, our experiment demonstrates that combining a cancer therapeutic vaccine with an immunostimulant, such as a 4-1BB agonist, can lead to greater efficacy in cancer treatment.

3. Discussion and Conclusions

The objective of this study is to enhance the efficacy of SVN-based vaccines for therapeutic purposes by investigating ROP-SVN, a variant vaccine design derived from WT-SVN. Our findings, both from in silico immune epitopes prediction and wet-lab experiments demonstrate that ROP-SVN is highly immunogenic. ROP-SVN contains more MHC class I and class II epitopes (Figure 2). ROP-SVN is capable of inducing significant specific

© 2023 The Authors. Advanced Therapeutics published by Wiley-VCH GmbH

23663987, 0, Downloaded from https://onlinelibrary.wiley.com/doi/10.1002/adtp.202300253 by Test, Wiley Online Library on [23/08/2023]. See the Terms and Conditions (https://onlinelibrary.wiley.com/terms-and-conditions) on Wiley Online Library for rules of use; OA articles are governed by the applicable Creative Commons License

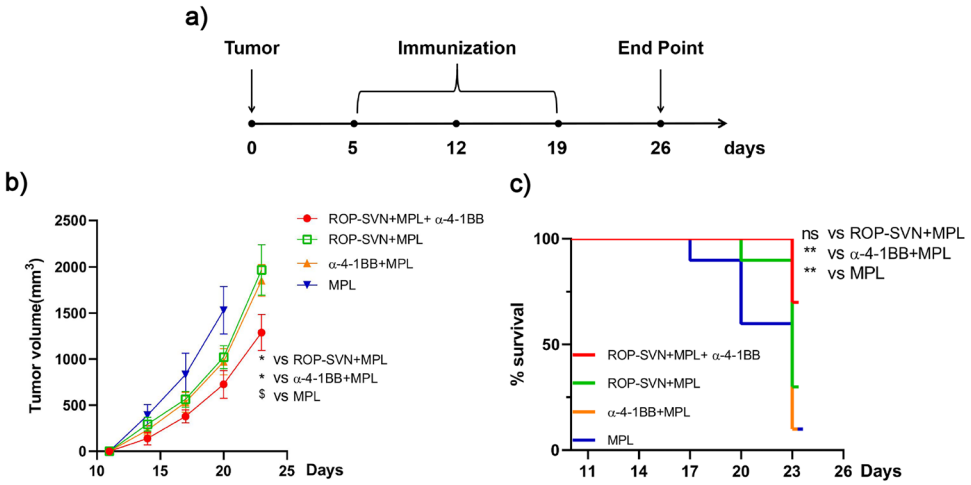

Figure 6. Evaluation of rescue from melanoma tumors in mice (N = 10 in each group) after immunization, in conjunction with α−4-1BB agonists. a) Schematic plan of immunization in melanoma-bearing mice. C57/BL mice were introduced with B16-SVN cells to develop melanoma tumors in vivo and immunized by ROP-SVN/MPL/α−4-1BB, ROP-SVN/MPL, α−4-1BB/MPL and MPL three times on day 5, 12 and 19 and sacrificed no later than 4 weeks after the induction of tumors by B16-SVN cells. b) Measurement of tumor volumes, in mm^3, every 3 days after immunization until day 23 due to tumor growth exceeding the ethical limit of 1500 mm^3. ROP-SVN/MPL/α−4-1BB were compared with ROP-SVN/MPL, α−4-1BB/MPL on day 23 and with MPL on day 20 before half of any mice group was lethal. \$ $p < 0.05$, \$\$ $p < 0.01$ and \$\$\$ $p < 0.001$ on day 20; *$p < 0.05$, **$p < 0.01$ and ***$p < 0.001$ on day 23; ns (not shown), not significant. c) Monitoring of percentage survival till day 23 as presented in a Kaplan–Meier plot. Statistical analysis was performed by comparing ROP-SVN/MPL/α−4-1BB to ROP-SVN/MPL, α−4-1BB/MPL and MPL, respectively. *$p < 0.05$; **$p < 0.01$; ***$p < 0.001$; ns, not significant. All data were presented as mean ± SEM.

cytotoxicity (46.5%) against SVN-bearing tumor cells by three times higher than that triggered by WT-SVN in vitro (Figure 4d). In contrast to humoral responses, which are similar between ROP-SVN and WT-SVN (Figure 4c and Figure 5e), ROP-SVN induces robust cell-mediated immune responses. This is consistent with our previous finding that protein was co-localized with the lysosome, while overlapping peptides were found in either lysosome or cytosol, an essential premise for cytosolic cross-presentation[9] (Figure S1, Supporting Information). In this case, ROPs are more likely to be cross-presented onto MHC class I molecules, triggering activation of CD8+ T cells and anti-cancer cytotoxicity (Figure S2, Supporting Information).

To establish an in vivo model, we inoculated B16-SVN cells into mice and allowed them to develop tumors of at least 2 mm in size, which is comparable to clinically detectable tumors. Our results provide compelling evidence that treatment with ROP-SVN/MPL led to a substantial reduction in tumor size and improved survival rates in mice with melanoma tumors (Figure 5b and c).

Conventionally, developing single peptide vaccines requires epitope mapping using overlapping peptide libraries.[7] Then, an epitope is identified in context with a specific MHC molecule, for instance, K^d, D^d, I-A^d in mice. Such epitope identification is time-consuming and labor intensive. Compared to single SVN peptides that have MHC restriction, the ROP construct comprises multiple sequential peptide sequences that overlap with each peptide's adjacent sequences, resulting in the inclusion of all possible T cell epitopes in the construct. This approach satisfies MHC polymorphism and activates both MHC class I and II pathways.[10] Additionally, the use of Cathepsin S protease-sensitive linkers (LRMK) between neighboring peptide sequences enables cleavage by Cathepsin S protease inside APCs to generate an overlapping peptide pool that can bind to MHC molecules for presentation. Furthermore, the ROP vaccine, which includes all potential epitopes in one single chain, is more cost-effective to produce and easier to regulate for marketing than the generation of multiple epitope peptide chains for a single target antigen.[33] Moreover, the ROP construct lacks the conformational structure of native antigens, which often include oncoproteins and other undesirable functions.

Based on the in-silico epitope analysis of ROP-SVN, there is a possibility that the vaccine could potentially induce an epitope shift by targeting the inserted enzyme substrate sequence (Figure 2). However, our wet-lab experiments have produced contrasting results. We have observed that the immune response generated by ROP-SVN remains robust when exposed to wild-type SVN or SVN-bearing tumor cells (Figure 4b,d, Figure 5d and Figure 6). These findings strongly suggest a minimal or negligible epitope shift. This observation may be attributed to the predominant presence of wild-type MHC class I epitopes.

Regarding predicted MHC class II-restricted epitopes (Figure 2b), it is important to note that all of them, whether derived from the wild-type or non-wild-type sequences, contribute to the overall immunogenicity against SVN-bearing tumor cells.

It is worth noting that ROPs have the capability to stimulate multiple clones of both CD4+ and CD8+ T cells, further supporting their immunogenic potential. In order to gain further insights into the characteristics of epitope-specific clones, we plan to include the measurement of SVN-specific T cell repertoire as part of our future experimental endeavors. This additional analysis will provide valuable information regarding the diversity and specificities of T cells responding to the ROP-SVN vaccine.

SVN can serve as a model TAA for examining recombinant overlapping peptides, as 33 common cancers are characterized by high SVN expression with biological significance (Figure 1). The such cancer-associated expression describes SVN as a novel

© 2023 The Authors. Advanced Therapeutics published by Wiley-VCH GmbH

23663987, 0, Downloaded from https://onlinelibrary.wiley.com/doi/10.1002/adtp.202300253 by Test, Wiley Online Library on [23/08/2023]. See the Terms and Conditions (https://onlinelibrary.wiley.com/terms-and-conditions) on Wiley Online Library for rules of use; OA articles are governed by the applicable Creative Commons License

23663987, 0, Downloaded from https://onlinelibrary.wiley.com/doi/10.1002/adtp.202300253 by Test, Wiley Online Library on [23/08/2023]. See the Terms and Conditions (https://onlinelibrary.wiley.com/terms-and-conditions) on Wiley Online Library for rules of use; OA articles are governed by the applicable Creative Commons License

vaccine target that can be developed into a platform of universal cancer vaccination, implying broader therapeutic applications.

Although the strong correlation that anti-tumor efficacies were attributed to ROP design was previously explained by enhanced cross-presentation,[8,30] its detailed mechanism remains a lack of investigation. It has been previously reported that a lack of cross-presentation via the vacuolar pathway was found in Cathepsin S-deficient mice,[34] suggesting that Cathepsin S protease is responsible for generating peptides to be presented on MHC class I molecules. Meanwhile, Cathepsin S protease-sensitive linkers (LRMK) in ROPs allow cleavage into overlapping peptides in the endosome of APCs. Thus, these peptides may become favorable for MHC class I antigen presentation. The specificity of Cathepsin S-cleaved peptides in binding to MHC class I molecules is still questionable and requires further assessment.

In addition, MPL adjuvants were co-administered with ROP vaccines to further enhance vaccine efficacy. MPL is derived and modified from the purified lipopolysaccharide (LPS) found in the cell wall of *Salmonella enterica*, making it a successful agonist for mouse Toll-like receptor (TLR)4, which activates dendritic cells.[35] The elevated levels of activated dendritic cells can boost ROP-mediated cross-presentation via increased complex formation between MHC class I molecules and antigenic vaccine peptides. MPL was advantageous to be coupled with ROP vaccines in this study due to its immunogenic profiling in mice.[36] However, it only functions as a partial TLR4 agonist in humans.[36] Moreover, activation of dendritic cells does not guarantee direct causation to enhanced cross-presentation and CD8+ cytotoxic T-cell immunity. Other adjuvants should be considered to replace MPL with more effective roles in promoting cross-presentation and interaction with ROP vaccines for clinical assessments.

After injecting mice with B16-SVN melanoma cells followed by immunization, there was an 8-fold decrease in the frequency of IFN-γ-producing T cells, compared to mice without B16-SVN cell injections. This unexpected drop may be associated with the immunosuppressive mechanisms of tumors. For instance, tumor cells can overexpress indoleamine 2,3-dioxygenase to break down tryptophan required for T cell proliferation or upregulate inhibitory receptors like PD-1 to deactivate T cells, leading to a failure to secrete IFN-γ.[37] Furthermore, effective T cells can home in on tumor sites[38] and become less concentrated in the spleen. In this case, the in vivo melanoma mice model was supplemented with additional administration of agonistic antibodies against 4-1BB, which emerged as a costimulatory signal on T cells to compensate for the excessive inhibitory signals from tumor cells, pushing the balance toward CD8+ T cell expansion.[39] This is consistent with the discovery of reduced tumor size and prolonged survival with 4-1BB to 80% at day 23 (Figure 6b and c).

It was observed that mice with B16-SVN melanoma and larger tumors (> 1000 mm^3) expressed significantly lower levels of SVN than those with smaller tumors (< 1000 mm^3) (Figure 5f, right). This finding suggests that therapeutic approaches involving ROP-SVN/MPL or WT-SVN/MPL may exert selection pressure on tumor cells, leading to increased survival and proliferation of cells expressing low levels of SVN and thereby becoming resistant to vaccination. This highlights the importance of personalized therapy, or precision medicine, by emphasizing the need for screening patients for their pathogenic profiles to maximize the benefits of tailored treatments. Combination therapy with a cocktail of anti-tumor agents with different mechanisms may also be a wise approach.

The observation that vaccination can act as a selection pressure is consistent with the immediate growth of tumors after the termination of vaccine immunization, wherein B16-SVN melanoma cells that have adapted to survive with low levels of SVN expression can evade vaccine-induced immunity and proliferate exponentially. It is crucial to acknowledge the rapidity of mutations and genomic instability in these tumor cells, which can generate heterogeneity and resistance within just a few days of treatment.

While ROP vaccines alone may be insufficient for triggering robust sterilized efficacy against tumors, combining them with α−4-1BB antibodies or other anti-cancer immunological agents can potentially boost immune responses and eradicate tumor cells before they develop resistance and continue to proliferate.

Overall, this study has demonstrated the potential of ROP-SVN vaccination by assessing its cytotoxic immune responses and anti-tumor efficacy, as well as its additional effect when combined with α−4-1BB antibodies in melanoma mice models. To accelerate the advancement of cancer vaccine development, attempts to combine ROP vaccines with immunostimulants or immune checkpoint inhibitors should be further pursued and examined to improve therapeutic efficacy in triggering specific immunity in the future.

4. Experimental Section

Bioinformatics Analyzing BIRC5 Expression Pattern in Human Pan-Cancer: To address the significance of SVN dysregulation in cancers, bioinformatic approaches were performed to investigate the *BIRC5* expression in various types of cancer by using TCGA tumor data compared to the control data for normal tissues from the GTEx project at UCSC Xena platform.[31,32] At UCSC Xena platform, RNA sequencing data were analyzed from 15 776 samples of 33 different cancer types, as presented in Figure 1. All expression data were normalized via log2 conversion.

Prediction of Immune Epitope Sequence Loaded to MHC Class Molecules: The MHC-binding T cell immune epitope for both WT-SVN and ROP-SVN was predicted at IEDB Analysis Resource. MHC class I or II sequences were separately analyzed using IEDB recommended 2020.09 (NetMHCpan EL 4.1) or 2023.05 (NetMHCIIpan 4.1 EL) in the context of mouse MHC class I (H-2-Db and H-2-Kb) or MHC class II (H2-IAb), respectively. Prediction score > 0.2 for MHC class I and > 0.1 for MHC class II was considered as high binding affinity to MHC class molecules.

B16-F10 Cell Culture and Transfection: B16-F10 murine melanoma cells were cultured in RPMI 1640 media (Solarbio, China) containing 100 IU mL^{-1} penicillin and 100 mg mL^{-1} streptomycin, supplemented with 10% heat-inactivated fetal bovine serum (FBS) (ExCell Bio, China), and incubated in a humidified atmosphere containing 5% CO_2 at 37 °C. The pET32a-GFP-SVN plasmid, essentially containing genes expressing GFP, hSVN and resistance to G418 antibiotic, was constructed as described by Cai et al.[10] GFP-hSVN stably transfected B16-F10 cell line, named B16-SVN, was established by Shanghai Model Organisms Center, Inc. (China). B16-SVN cells were tested by PCR, following agarose gel electrophoresis and western blot to confirm the overexpression of GFP-hSVN (1100 bp: forward primer, ATGGGAGCACCTACACTGCC; reverse primer, TTACTTGTACAGCTCGTCCA), and later introduced to mice to establish in vivo melanoma model.

Generation of WT-SVN and ROP-SVN: Synthetic cDNA genes were designed with codon selection optimized for expression in *E. coli* and synthesized by GeneArt (Thermo, UK) to encode ROP-SVN (33.81 kDa: MGAPTLPPAWQPFLKDHRISTFKNWPFLEGLRMKD HRISTFKNWPFLEGCACTPERMAEAGFIHLRMKACTPERMAEAGFIHCPTE

© 2023 The Authors. Advanced Therapeutics published by Wiley-VCH GmbH

NEPDLAQCFFLRMKPTENEPDLAQCFFCFKELEGWEPDDDPIELRMKFKE LEGWEPDDDPIEEHKKHSSGCAFLSVKLRMKEHKKHSSGCAFLSVKKQFE ELTLGEFLKLRMKQFEELTLGEFLKLDRERAKNKIAKETNNKLRMKRERAKN KIAKETNNKKKEFEETAEKVRRAILRMKKEFEETAEKVRRAIEQLAAMD) or WT-SVN (17.6 kDa, while the length is detected as 22.0 kDa due to manual analysis in the reality:[40] MGAPTLPPAWQPFLKDHRISTFKNW-PFLEGCACTPERMAEAGFIHCPTENEPDLAQCFFCFKELEGWEPDDDPIEE HKKHSSGCAFLSVKKQFEELTLGEFLKLDRERAKNKIAKETNNKKKEFEETA KKVRRAIEQLAAMD[41]). Molecular cloning of ROP-SVN and WT-SVN cDNAs was performed as described by Cai et al,[10] to obtain *E. coli* BL21 (DE3) clones positive for transfection.

Transformed BL21 (DE3) colonies were individually picked into LB broth (Solarbio, China) with 50 μg mL^{-1} kanamycin (Solarbio, China) and those expressing ROP-SVN were cultured overnight at 37 °C, while others that expressed WT-SVN were shaken at the speed of 150 rpm at 15 °C overnight. The overnight culture was then diluted 100 times with fresh LB and repeated culturing until the OD value detected by UV1700 Single Beam Spectrophotometer (Yoke, China) at a wavelength of 600 nm reached 0.6. BL21 (DE3) cells were induced by 0.5 mM Isopropyl-beta-D-thiogalactopyranoside (IPTG) (Solarbio, China), harvested after 16 h by centrifugation at a rate of 4500 rpm in 4 °C for 30 min, resuspended in lysis buffer (50 mM Tris-HCl, pH7.5) and lysed by sonication, during which number 8 ultrasonic probe is selected with 60% power, 3s on, 3s off for 40 cycles. To collect WT-SVN, supernatants, where the soluble proteins dissolved, were collected after centrifugation at 20 000 g for 45 min, purified by incubating with nickel affinity chromatography using Ni Smart Beads 6FF (SMART Lifesciences, China) for 30 min, washed with 30 resin volumes of lysis buffer and eluted with lysis buffer containing 300 mM imidazole (Solarbio, China). Debris of ROP-SVN peptides that formed inclusion bodies and became insoluble, was re-suspended in 50 mM phosphate buffer (8 M urea and 0.2 M NaCl, pH 7.4) and centrifuged at 20 000 g for 45 min, following similar purification and elution using 50 mM phosphate buffer (8 M urea, 0.2 M NaCl and 300 mM imidazole, pH 7.4). To refold ROP-SVN peptides, eluted proteins were transferred to a dialysis bag (< molecular weight 3.5 kDa), which was then immersed into dialysate buffer 1 (4 M urea, 100 mM acetic acid, pH 3.0), then to dialysate buffer 2 (20 mM acetic acid, pH 3.0), finally to dialysate buffer 3 (20 mM acetic acid, pH 4.5). One μg of each purified peptide, with a 14.4–97.4 kD protein marker (Solarbio, China), was analyzed using an SDS-PAGE gel kit (Solarbio, China), according to the manufacturer's instructions.

Immunization of Mice and Melanoma Model: Specific pathogen-free six-week-old female C57BL/6 mice were purchased from the Jiangsu Aniphe Biolaboratory Inc. and were handled following the international guidelines required for experimentation with animals.[42] Mice experiments were approved by the General Hospital of Tianjin Medical University, Tianjin, China (Approval Number: SCXK (Jin) 2020-0017). To examine the immune response induced by ROP-SVN, six C57BL/6 mice per experimental group were injected subcutaneously with 100 μg of ROP-SVN or WT-SVN emulsified with 50 μL of MPL (Sigma, USA), an adjuvant essential for boosting the efficacy of vaccination. Mice injected with MPL adjuvant were used as controls. They were boosted subcutaneously twice at 2-week intervals with the same vaccines emulsified with MPL. Two weeks after the last boost, all mice were sacrificed to perform the detection and analysis of cellular and humoral immune responses.

For experiments that assess the anti-tumor effect of ROP-SVN, each C57BL/6 mouse was injected subcutaneously with 1.5×10^5 viable B16-SVN cells at the right lower thigh on day 0 and monitored daily until a melanoma tumor ≥ 2 mm in diameter with progressive growth was observed. Ten C57BL/6 mice that carried in vivo melanoma tumors in each experimental group were injected subcutaneously with 100 μg of ROP-SVN or WT-SVN emulsified with 50 μL of MPL. Mice injected with MPL adjuvant or/and PBS (Solarbio, China) were used as controls. They were boosted subcutaneously on days 5, 12, and 19. Tumor diameters were measured as width and length every 3 days with a caliper and volume was calculated using the formula: (length × $width^2$) / 2 (mm^3). Percentage survival was examined as live mice count/total count × 100%. Mice were sacrificed due to ethical limits of 1500 mm^3 or no later than day 26 after inoculation with B16-SVN cells, and the tumors were extracted, weighed, snap-frozen in liquid nitrogen, and stored at −80 °C.

Additional experiments that furthered the anti-tumor investigation included tumor volume and percentage survival calculations in another ten melanoma-bearing C57BL/6 mice per group after weekly subcutaneous injection with 100 μg of ROP-SVN with MPL adjuvant and intraperitoneal injection at 3-day intervals with 0.6 mg kg^{-1} of an anti-mouse 4-1BB monoclonal antibody (Bio X Cell, USA), that was well-documented with its anti-tumor immunostimulant by inducing expansion and differentiation of polyclonal tumor-specific CD8+ T cells.[43–45] Mice that were injected with 0.6 mg kg^{-1} of mice α−4-1BB plus 50 μL MPL and MPL adjuvant only were used as controls.

Enzyme-Linked Immunosorbent Spot (ELISpot) Assays: Upon sacrifice, splenocytes were separated and purified by adapting the Ficoll-Hypaque density gradient centrifugation approach[46]. In detail, all mouse spleens were meshed and loaded into mouse lymphocyte separation medium (Solarbio, China), and centrifuged at 1000 g for 22 min to collect layered lymphocytes that were then transferred to a new tube of cell culture medium. The separated spleen cells were washed by FBS-free medium, seeded 1×10^5 splenocytes/well and incubated overnight with 5 μg mL^{-1} SVN protein in anti-IFN-γ-Ab precoated plates (Millipore, Bedford, MA). After the removal of cells and proteins, biotinylated anti-IFNγ antibodies (Mebtech, Swede) were incubated in a ratio of 1 in 1000 with PBS containing 0.5% bovine serum albumin (BSA) (Sigma, USA) for 2 h at room temperature, followed by another 1 h of incubation at room temperature with an enzyme-labelled anti-biotin antibody (Mebtech, Swede) diluted in 1 in 1000 by PBS with 0.5% BSA. Finally, 5-bromo-4-chloro-3'-indolyphosphate and nitro-blue tetrazolium (BCIP/NBT) (Thermo, USA) was used for color development, and the reaction was terminated by washing plates with tap water and plates were air-dried. Spots were counted with ImmunoSpot® S6 Entry M2 (CTL, USA). Results were expressed as spot-forming units/10^6 cells.

Cytotoxicity Assay: Cytotoxicity was further confirmed as CTL activity by using previous protocols for CTL cytotoxicity assay[47–49]. Splenocytes from immunized mice were co-cultured with 1×10^4 B16-SVN cells in RPMI 1640 media (Solarbio, China) with 3% BSA, at the E:T ratio of 50 or 100 to 1, in an incubator for 4 h at 37 °C. The supernatant was incubated with an LDH detection mixture in the darkness for 30 min and terminated with a Stop solution in CyQUANT™ LDH Cytotoxicity Assay kit (Invitrogen, USA). OD value was measured at a wavelength of 490 nm using a Multiskan™ FC Microplate Photometer (Thermo, USA). B16-SVN cells or splenocytes alone indicate spontaneous cytotoxicity and B16-SVN cells lysed by 9% Triton X-100 served as maximum cytotoxicity. The percentage of CTL activity was calculated as specific cytotoxicity (%) = $[(OD_{sample} - OD_{spontaneous})/ (OD_{maximum} - OD_{spontaneous})] \times 100\%$.

Enzyme-Linked Immunosorbent Assay (ELISA): Serums of all mice were collected to identify the titers of anti-SVN antibodies detected in immunized mice. Ninety-six well plates were coated with SVN protein in 2 μg mL^{-1} PBS overnight at 4°C and washed 5 times with PBS containing 0.05% Tween-20 (PBST). SVN-coated wells were blocked with 5% BSA in PBS at 37 °C for 2 h and then incubated with individual serum samples that were previously diluted with PBS in 1 in 10^3, 10^4 and 10^5 at 37 °C for another hour. Serums were washed off by PBS in wells, which were subsequently incubated with HRP-conjugated anti-mouse antibodies (Abcam, UK) in 1 in 10 000 with PBS at 37 °C for 45 min and washed with PBST. To visualize the reactions, 3,3',5,5'- tetramethylbenzidine solution (TMB) (Solarbio, China) was added to wells to trigger a color development, which after 5 min, was terminated by adding 2 M H_2SO_4 (Solarbio, China). OD value was detected at a wavelength of 450 nm using a Multiskan™ FC Microplate Photometer (Thermo, USA). Titers were determined as the maximum serum dilution, in which the OD value is greater than 0.2 as the detectability baseline for anti-SVN antibody.[50]

Double-Antibody Sandwich Enzyme-Linked Immunosorbent Assay (DAS-ELISA): To quantify SVN protein expression in immunized mice melanoma, extracted tumors per gram were mixed with 5 mL RIPA buffer (Beyotime, China) supplemented with 2× protease inhibitors (Beyotime, China), and then homogenized on the ice for 30 min, followed by centrifugation for 20 min at 12000 g at 4 °C. Supernatants were collected and

© 2023 The Authors. Advanced Therapeutics published by Wiley-VCH GmbH

23663987, 0, Downloaded from https://onlinelibrary.wiley.com/doi/10.1002/adtp.202300253 by Test, Wiley Online Library on [23/08/2023]. See the Terms and Conditions (https://onlinelibrary.wiley.com/terms-and-conditions) on Wiley Online Library for rules of use; OA articles are governed by the applicable Creative Commons License

stored at 4 °C for later analysis. Total protein concentrations were determined using the BCA protein assay kit (Solarbio, China) according to the manufacturer's description. Ninety-six well plates were coated with 100 µL of 5 µg mL^{-1} capture antibody and stored at 4 °C overnight. Following washing 5 times with PBST, coated wells were blocked with 5% BSA/PBS at room temperature for 2 h. Wells were washed similarly and incubated with serial 2-fold dilutions of purified SVN protein from 1.8 to 1,000 ng mL^{-1} and supernatant of tumor lysate at 4 °C for 2 h and then washed off by PBST. Wells were then incubated with HRP-conjugated detective antibodies diluted 10 000 times at room temperature for 1 h. After washing, TMB was added to wells to trigger a color development, which after 5 min, was terminated by adding 2 M H_2SO_4 (Solarbio, China). The absorbance of plates was detected at a wavelength of 450 nm using a Multiskan™ FC Microplate Photometer (Thermo, USA). Concentrations of tumor SVN were determined by referring to the standard curved plotted by OD values of serially diluted SVN with known concentrations and standardized to each tumor gram.

Statistical Analysis: All in vivo and in vitro experiments were performed at least 3 times. Data were presented as mean ± SEM. Differences between the groups were assessed for statistical significance using the two-tailed unpaired T-test analysis. $p < 0.05$ was considered significant, and $p < 0.01$ was considered highly significant. All statistical analyses were performed with GraphPad Prism 8.0.2 software.

Supporting Information

Supporting Information is available from the Wiley Online Library or from the author.

Acknowledgements

The authors declare that this study received funding from Oxford Vacmedix UK Ltd. and the Chinese National Natural Science Funding program (81771221, 81870967 and 82071384). The funding subjects did not involve in the process of study design and performance, data interpretation and analysis, writing and revision of this article or decisions on submission and publication.

Conflict of Interest

The authors declare a potential conflict of interest that Q. Zhang, Q. Zheng, W. Lu and S. Jiang are employees and/or shareholders of Oxford Vacmedix Ltd which develops cancer vaccines. The rest authors declare the absence of any commercial or financial relationships that could be construed as a potential conflict of interest.

Author Contributions

Y.Z. and Y.Z. contributed equally to this work and should be considered joint first authorship. Both were mainly responsible for the literature search, experimental manipulations, analysis and interpretation, and writing and revision. The rest conducted most of the proposal, conceptualism, and some experimental setup and revision. All authors contributed to the article and approved the submitted version.

Data Availability Statement

The TCGA and GTEx databases analyzed during the current study are available in the UCSC Xena platform repository, http://xena.ucsc.edu/.[31,32] The IEDB recommended 2020.09 (NetMHCpan EL 4.1) or 2023.05 (NetMHCIIpan 4.1 EL) are available in IEDB Analysis Resource, http://tools.immuneepitope.org/mhci/ and http://tools.iedb.org/mhcii/, respectively. Other data that support the findings of this study are available on request from the corresponding author.

Keywords

cancer immunotherapy, cross-presentation, melanoma, peptide-based vaccination, recombinant overlapping peptides, survivin

Received: July 15, 2023
Published online:

[1] H. Sung, J. Ferlay, R. L. Siegel, M. Laversanne, I. Soerjomataram, A. Jemal, F. Bray, *Ca-Cancer J. Clin.* **2021**, *71*, 209.
[2] C. H. Huber, T. Wolfel, *J. Cancer Res. Clin. Oncol.* **2004**, *130*, 367.
[3] A. J. Stephens, N. A. Burgess-Brown, S. Jiang, *Front Immunol.* **2021**, *12*, 696791.
[4] E. Schneble, G. T. Clifton, D. F. Hale, G. E. Peoples, *Meth. Molec. Bio.* **2016**, *1403*, 797.
[5] S. Kelderman, P. Kvistborg, *Biochim. Biophys. Acta* **2016**, *1865*, 83.
[6] F. Li, I. Aljahdali, X. Ling, *J. Exp. Clin. Cancer Res.* **2019**, *38*, 368.
[7] S. Jiang, N. J. Borthwick, P. Morrison, G. F. Gao, M. W. Steward, *J. Gen. Virol.* **2002**, *83*, 429.
[8] S. Jiang, R. Song, S. Popov, S. Mirshahidi, R. M. Ruprecht, *Vaccine* **2006**, *24*, 6356.
[9] H. Zhang, H. Hong, D. Li, S. Ma, Y. Di, A. Stoten, N. Haig, K. Di Gleria, Z. Yu, X. N. Xu, A. McMichael, S. Jiang, *J. Biol. Chem.* **2009**, *284*, 9184.
[10] L. Cai, J. Zhang, R. Zhu, W. Shi, X. Xia, M. Edwards, W. Finch, A. Coombs, J. Gao, K. Chen, S. Owen, S. Jiang, W. Lu, *Oncotarget* **2017**, *8*, 76516.
[11] E. Tchilian, D. Ahuja, A. Hey, S. Jiang, P. Beverley, *Vaccine* **2013**, *31*, 4624.
[12] Y. Li, W. Lu, J. Yang, M. Edwards, S. Jiang, *Expert Opin. Biol. Ther.* **2021**, *21*, 1429.
[13] G. Ambrosini, C. Adida, D. C. Altieri, *Nat. Med.* **1997**, *3*, 917.
[14] P. K. Jaiswal, A. Goel, R. D. Mittal, *Indian J. Med. Res.* **2015**, *141*, 389.
[15] H. Garg, P. Suri, J. C. Gupta, G. P. Talwar, S. Dubey, *Cancer Cell Int.* **2016**, *16*, 49.
[16] Y. L. Yang, X. M. Li, *Cell Res.* **2000**, *10*, 169.
[17] L. Huang, G. Chen, Y. Chen, W. Wu, C. Tao, H. Shao, S. Huang, H. Shen, *Anti-Cancer Drugs* **2021**, *32*, 138.
[18] X. Jiang, S. Guan, Y. Qiao, X. Li, Y. Xu, L. Yang, Z. Kuai, H. Zhang, Y. Shi, W. Kong, Y. Shan, H. Zhang, *J. Cell. Physiol.* **2018**, *233*, 4926.
[19] N. J. Nitschke, J. Bjoern, T. Z. Iversen, M. H. Andersen, I. M. Svane, *Stem Cell Investig.* **2017**, *4*, 77.
[20] M. S. Ahluwalia, D. A. Reardon, A. P. Abad, W. T. Curry, E. T. Wong, S. A. Figel, L. L. Mechtler, D. M. Peereboom, A. D. Hutson, H. G. Withers, S. Liu, A. N. Belal, J. Qiu, K. M. Mogensen, S. S. Dharma, A. Dhawan, M. T. Birkemeier, D. M. Casucci, M. J. Ciesielski, R. A. Fenstermaker, *J. Clini. Oncol.: Off. J. Ameri. Soc. Clin. Oncol.* **2023**, *41*, 1453.
[21] P. M. Galbo, Jr., M. J. Ciesielski, S. Figel, O. Maguire, J. Qiu, L. Wiltsie, H. Minderman, R. A. Fenstermaker, *Oncotarget* **2017**, *8*, 114722.
[22] Z. Khan, A. A. Khan, G. B. Prasad, N. Khan, R. P. Tiwari, P. S. Bisen, *J. Eur. Soc. for Therap. Radiol. and Oncol.* **2016**, *118*, 359.
[23] Z. Khan, N. Khan, R. P. Tiwari, I. K. Patro, G. B. Prasad, P. S. Bisen, *J. Eur. Soc. for Therap. Radiol. and Oncol.* **2010**, *96*, 267.
[24] M. Mikulandra, A. Kobescak, B. Verillaud, P. Busson, T. Matijevic Glavan, *Cellular oncology (Dordrecht)* **2019**, *42*, 29.
[25] P. Bertino, M. Panigada, E. Soprana, V. Bianchi, S. Bertilaccio, F. Sanvito, A. H. Rose, H. Yang, G. Gaudino, P. R. Hoffmann, A. Siccardi, M. Carbone, *Int. J. Cancer* **2013**, *133*, 612.

© 2023 The Authors. Advanced Therapeutics published by Wiley-VCH GmbH

23663987, 0, Downloaded from https://onlinelibrary.wiley.com/doi/10.1002/adtp.202300253 by Test, Wiley Online Library on [23/08/2023]. See the Terms and Conditions (https://onlinelibrary.wiley.com/terms-and-conditions) on Wiley Online Library for rules of use; OA articles are governed by the applicable Creative Commons License

[26] P. R. Hoffmann, M. Panigada, E. Soprana, F. Terry, I. S. Bandar, A. Napolitano, A. H. Rose, F. W. Hoffmann, L. C. Ndhlovu, M. Belcaid, L. Moise, A. S. De Groot, M. Carbone, G. Gaudino, T. Matsui, A. Siccardi, P. Bertino, *Hum Vaccin. Immunother.* **2015**, *11*, 1585.
[27] Q. Wang, R. Shu, H. He, L. Wang, Y. Ma, H. Zhu, Z. Wang, S. Wang, G. Shen, P. Lei, *Internat. J. Oncol.* **2012**, *41*, 652.
[28] D. E. Zhu, N. Höti, Z. Song, L. Jin, Z. Wu, Q. Wu, M. Wu, *Cancer Gene Ther.* **2006**, *13*, 762.
[29] R. E. Hollingsworth, K. Jansen, *NPJ Vaccines* **2019**, *4*, 7.
[30] P. Sabbatini, T. Tsuji, L. Ferran, E. Ritter, C. Sedrak, K. Tuballes, A. A. Jungbluth, G. Ritter, C. Aghajanian, K. Bell-McGuinn, M. L. Hensley, J. Konner, W. Tew, D. R. Spriggs, E. W. Hoffman, R. Venhaus, L. Pan, A. M. Salazar, C. M. Diefenbach, L. J. Old, S. Gnjatic, *Clin. Cancer Res.* **2012**, *18*, 6497.
[31] M. J. Goldman, B. Craft, M. Hastie, K. Repečka, F. McDade, A. Kamath, A. Banerjee, Y. Luo, D. Rogers, A. N. Brooks, J. Zhu, D. Haussler, *Nat. Biotechnol.* **2020**, *38*, 675.
[32] J. Vivian, A. A. Rao, F. A. Nothaft, C. Ketchum, J. Armstrong, A. Novak, J. Pfeil, J. Narkizian, A. D. Deran, A. Musselman-Brown, H. Schmidt, P. Amstutz, B. Craft, M. Goldman, K. Rosenbloom, M. Cline, B. O'Connor, M. Hanna, C. Birger, W. J. Kent, D. A. Patterson, A. D. Joseph, J. Zhu, S. Zaranek, G. Getz, D. Haussler, B. Paten, *Nat. Biotechnol.* **2017**, *35*, 314.
[33] J. Greenbaum, J. Sidney, J. Chung, C. Brander, B. Peters, A. Sette, *Immunogenetics* **2011**, *63*, 325.
[34] L. Shen, L. J. Sigal, M. Boes, K. L. Rock, *Immunity* **2004**, *21*, 155.
[35] A. M. Didierlaurent, C. Collignon, P. Bourguignon, S. Wouters, K. Fierens, M. Fochesato, N. Dendouga, C. Langlet, B. Malissen, B. N. Lambrecht, N. Garcon, M. Van Mechelen, S. Morel, *J. Immunol.* **2014**, *193*, 1920.
[36] Y. Q. Wang, H. Bazin-Lee, J. T. Evans, C. R. Casella, T. C. Mitchell, *Front Immunol.* **2020**, *11*, 577823.
[37] Z. Zhang, S. Liu, B. Zhang, L. Qiao, Y. Zhang, Y. Zhang, *Front. Cell and Develop. Bio.* **2020**, *8*, 17.
[38] L. L. van der Woude, M. A. J. Gorris, A. Halilovic, C. G. Figdor, I. J. M. de Vries, *Trends in Cancer* **2017**, *3*, 797.
[39] D. S. Vinay, B. S. Kwon, *BMB Rep.* **2014**, *47*, 122.
[40] CLOUD-CLONE CORP.(CCC). Recombinant Survivin (Surv), http://www.cloud-clone.com/products/RPC045Hu01.html, (accessed: January 2023).
[41] T. U. Consortium, *Nucleic Acids Res.* **2022**, *51*, D523.
[42] N. Percie du Sert, V. Hurst, A. Ahluwalia, S. Alam, M. T. Avey, M. Baker, W. J. Browne, A. Clark, I. C. Cuthill, U. Dirnagl, M. Emerson, P. Garner, S. T. Holgate, D. W. Howells, N. A. Karp, S. E. Lazic, K. Lidster, C. J. MacCallum, M. Macleod, E. J. Pearl, O. H. Petersen, F. Rawle, P. Reynolds, K. Rooney, E. S. Sena, S. D. Silberberg, T. Steckler, H. Wurbel, *PLoS Biol.* **2020**, *18*, e3000410.
[43] J. A. Chacon, R. C. Wu, P. Sukhumalchandra, J. J. Molldrem, A. Sarnaik, S. Pilon-Thomas, J. Weber, P. Hwu, L. Radvanyi, *PLoS One* **2013**, *8*, e60031.
[44] Y. H. Kim, B. K. Choi, H. S. Oh, W. J. Kang, R. S. Mittler, B. S. Kwon, *Mol. Cancer Ther.* **2009**, *8*, 469.
[45] Q. Li, J. Ai, Z. Song, J. Liu, B. Shan, *Cell Mol. Immunol.* **2008**, *5*, 379.
[46] I. J. Fuss, M. E. Kanof, P. D. Smith, H. Zola, *Curr. Protoc. Immunol.* **2009**.
[47] H. Zhang, C. Liu, F. Zhang, F. Geng, Q. Xia, Z. Lu, P. Xu, Y. Xie, H. Wu, B. Yu, J. Wu, X. Yu, W. Kong, *Vaccine* **2016**, *34*, 2648.
[48] H. Zhang, Y. Wang, C. Liu, L. Zhang, Q. Xia, Y. Zhang, J. Wu, C. Jiang, Y. Chen, Y. Wu, X. Zha, X. Yu, W. Kong, *Cancer Immunol. Immunother.* **2012**, *61*, 1857.
[49] S. Zhang, H. Zhang, H. Shi, X. Yu, W. Kong, W. Li, *Hum Immunol.* **2008**, *69*, 250.
[50] S. A. Fuller, M. Takahashi, J. G. Hurrell, Immunization of mice, Current protocols in molecular biology, **2001**.

© 2023 The Authors. Advanced Therapeutics published by Wiley-VCH GmbH

23663987, 0, Downloaded from https://onlinelibrary.wiley.com/doi/10.1002/adtp.202300253 by Test, Wiley Online Library on [23/08/2023]. See the Terms and Conditions (https://onlinelibrary.wiley.com/terms-and-conditions) on Wiley Online Library for rules of use; OA articles are governed by the applicable Creative Commons License